Human Molecular Genetics, 2024, Vol. 33, 18, 1575–1583
https://doi.org/10.1093/hmg/ddae096
Advance access publication date 13 June 2024
Original Article

The maternal protein NLRP5 stabilizes UHRF1 in the cytoplasm: implication for the pathogenesis of multilocus imprinting disturbance

Motoko Unoki[1,2,*], Shuhei Uemura[2,3], Akihiro Fujimoto[1], Hiroyuki Sasaki[2]

[1]Department of Human Genetics, School of International Health, Graduate School of Medicine, The University of Tokyo, 7-3-1 Hongo, Bunkyo-ku, Tokyo 113-0033, Japan
[2]Division of Epigenomics and Development, Medical Institute of Bioregulation, Kyushu University, 3-1-1 Maidashi, Higashi-ku, Fukuoka-shi, Fukuoka 812-8582, Japan
[3]Department of Genome Biology, Graduate School of Medicine, Osaka University, 2-2 Yamadaoka, Suita-shi, Osaka 565-0871, Japan

*Corresponding author. Department of Human Genetics, School of International Health, Graduate School of Medicine, The University of Tokyo, 7-3-1 Hongo, Bunkyo-ku, Tokyo 113-0033, Japan. E-mail: unokim@m.u-tokyo.ac.jp

Abstract

We have recently discovered that the so-called subcortical maternal complex (SCMC) proteins composing of cytoplasmic lattices are destabilized in *Uhrf1* knockout murine fully grown oocytes (FGOs). Here we report that human UHRF1 interacts with human NLRP5 and OOEP, which are core components of the SCMC. Moreover, NLRP5 and OOEP interact with DPPA3, which is an essential factor for exporting UHRF1 from the nucleus to the cytoplasm in oocytes. We identify that NLRP5, not OOEP, stabilizes UHRF1 protein in the cytoplasm utilizing specifically engineered cell lines mimicking UHRF1 status in oocytes and preimplantation embryos. Further, UHRF1 is destabilized both in the cytoplasm and nucleus of *Nlrp5* knockout murine FGOs. Since pathogenic variants of the SCMC components frequently cause multilocus imprinting disturbance and UHRF1 is essential for maintaining CpG methylation of imprinting control regions during preimplantation development, our results suggest possible pathogenesis behind the disease, which has been a long-standing mystery.

Graphical Abstract

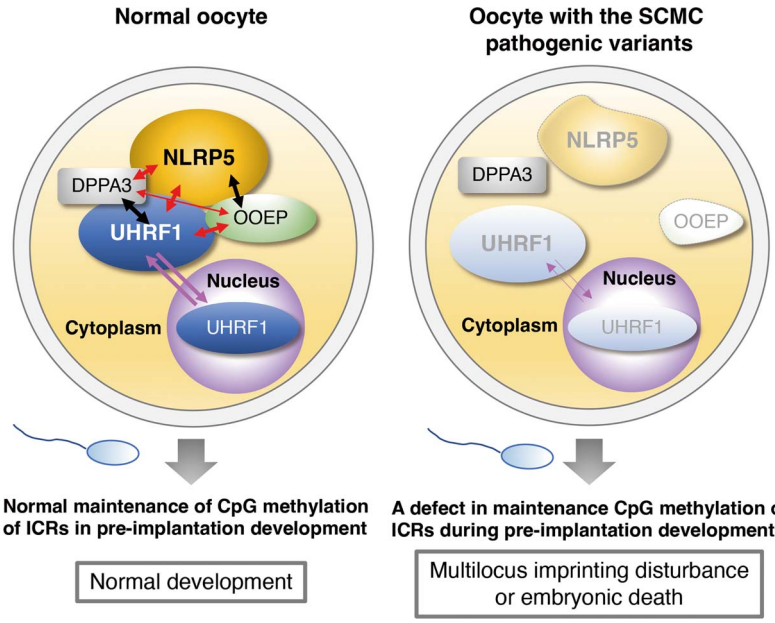

A model of molecular pathogenesis of multi-locus imprinting disturbance (MLID).

Keywords: UHRF1; NLRP5; multilocus imprinting disturbance; SCMC; MLID

Received: March 15, 2024. **Revised:** May 28, 2024. **Accepted:** May 30, 2024

Introduction

Genomic imprinting is an epigenetic process regulated by germline-derived DNA (CpG) methylation that is resistant to embryonic reprogramming, resulting in parental origin-specific monoallelic gene expression. Germ cell-specific CpG methylation including imprinting control regions (ICRs) is established by *de novo* DNA methyltransferases (DNMTs) during gametogenesis after it is genome-widely erased in primordial germ cells. After fertilization, CpG methylation is again genome-widely erased in preimplantation embryos. The demethylation mainly occurs passively due to the developmental stage-specific cytoplasmic localization of DNMT1 and ubiquitin-like with plant homeodomain (PHD) and really interesting new gene (RING) finger domains 1 (UHRF1), both of which usually locates in the nucleus and are essential for the maintenance of CpG methylation [1, 2]. However, exceptionally, the CpGs in the ICRs, which are differentially methylated by parental origin, are maintained by a small amount of the DNMT1/UHRF1 complex retained in the nucleus cooperating with Kruppel-associated-zinc finger proteins (KRAB-ZNFs), ZFP57 and ZNF445 [3].

Genomic imprinting is essential for normal development, and hypo- or hyper-CpG methylation of the imprinted loci causes various imprinting disorders (IDs). Multilocus imprinting disturbance (MLID) in a subset of patients with IDs is known to be caused by pathogenic variants of the KRAB-ZNFs or proteins in the so-called subcortical maternal complex (SCMC), whose core members are NACHT, LRR, and PYD domains-containing 5 (NLRP5), oocyte-expressed protein homolog (OOEP), transducin-like enhancer protein 6 (TLE6), and KH domain containing 3 like (KHDC3L) [4–7]. The pathogenic variants of these genes are also known to cause female infertility when embryos with the variants die before birth [8]. However, since homozygous males carrying these variants remain healthy and fertile [9], this would contribute to the allele frequency of these alleles in the human population. While ZFP57 and ZNF445 are nuclear proteins, the SCMC components compose the cytoplasmic lattices (CTLs) of oocytes [10]. Hence, it has been a mystery how these pathogenic variants of the SCMC proteins can cause CpG hypomethylation. There are two possible timings if any defects can cause hypomethylation of the CpGs in multiple ICRs. The first timing is during gametogenesis and the second timing is during preimplantation development. Since the SCMC components are specifically expressed in oocytes and preimplantation embryos [11], hypomethylation of the CpGs in the ICRs unlikely occurs during spermatogenesis. In addition, since both maternal and paternal ICRs are reported to be hypomethylated in MLID patients, CpG hypomethylation plausibly occurs due to a defect in the maintenance CpG methylation of ICRs against genome-wide demethylation in preimplantation development.

Recently, we have reported that UHRF1 is indispensable for preimplantation development; CTLs are not formed properly in *Uhrf1* knockout (KO) fully grown oocytes (FGOs), and expression of the SCMC components including NLRP5 (also known as Mater in mouse), OOEP (also known as FLOPED in mouse), TLE6, and KHDC3 (mouse homolog of KHDC3L, and also known as FILIA in mouse) was decreased at protein levels [12]. In addition, the subcellular localization of NLRP5 and OOEP are changed in *Uhrf1* KO FGOs. Intriguingly, the phenotype of *Uhrf1* maternal-KO and the SCMC (*Nlrp5*, *Ooep*, *Tle6*, and *Khdc3*) KO mice embryos are similar; all of them die during preimplantation development [2, 12–16]. In addition, recently, it has been reported that CTLs store UHRF1 both in murine and human oocytes [10]. Moreover, an MLID patient carried a heterozygous pathogenic variant of the *UHRF1* gene (c.514G>A, p.Val172Met) has been reported, although additional sporadic factors during development may be involved in the pathogenesis of this case [7]. Therefore, we hypothesized that there could be interactions between UHRF1 and the SCMC components.

In this article, we examined interactions between human UHRF1 and the SCMC core components, NLRP5, OOEP, TLE6, and KHDC3L. Among these proteins, we found that NLRP5 and OOEP interacted with UHRF1, and NLRP5 stabilized UHRF1 in the cytoplasm. We believe that our findings open a door for elucidating the mechanism of how pathogenic variants of the cytoplasmic proteins cause CpG hypomethylation.

Results

UHRF1 interacts with NLRP5 and OOEP among the four SCMC core components

Recently, we have discovered that protein levels, not mRNA levels, of the SCMC-associated proteins are decreased in *Uhrf1* KO murine FGOs [12] (Supplementary Material, Fig. S1A and B). Since pathogenic variants of the SCMC-associated proteins and *UHRF1* are found in patients with MLID and female infertility [4, 7], we hypothesized that interactions between UHRF1 and the SCMC proteins could contribute to their protein stability and disruption of the interactions may cause these diseases. Thus, we examined possible interactions between the four human SCMC core components, NLRP5, OOEP, TLE6, and KHDC3L, and human UHRF1 in human embryonic kidney (HEK) 293T cells. Among the SCMC core components, UHRF1 was coimmunoprecipitated (co-IPed) with FLAG-NLRP5 and FLAG-OOEP (Fig. 1A). Of note, since HEK293T cells do not express oocyte-specific proteins including the SCMC-associated proteins, the interaction between UHRF1 and NLRP5 or OOEP is likely direct.

It is well investigated that developmental pluripotency associated 3 (DPPA3, also known as PGC7 and STELLA) is an essential factor that binds to and exports UHRF1 from the nucleus to the cytoplasm during oocyte growth of mice [17, 18]. Intriguingly, the majority of DPPA3 relocates in the nucleus of oocytes by the germinal vesicle (GV) stage, in which UHRF1 remains to localize in the cytoplasm. Therefore, we hypothesized that after UHRF1 is exported by DPPA3 to the cytoplasm, the DPPA3-UHRF1 complex might interact with the SCMC proteins to hand UHRF1 over to them. We firstly confirmed the interaction between human UHRF1 and human DPPA3 (Fig. 1B). Then, we found that NLRP5 and OOEP also interact with DPPA3 (Fig. 1C). The interactions among NLRP5, OOEP, UHRF1, and DPPA3 determined by previous studies [15, 18, 19] and this study are schematically summarized in Fig. 1D.

UHRF1 interacts with NLRP5 and OOEP via multiple domains

UHRF1 is composed of five domains, which are a ubiquitin-like (UBL) domain, a tandem Tudor domain (TTD), a PHD, a su(var)3-9 enhancer-of-zeste and trithorax (SET) and RING-associated (SRA) domain, and a RING domain (Fig. 2A left). Among these domains, UHRF1 interacted with FLAG-NLRP5 and FLAG-OOEP via almost all domains (UBL, TTD, SRA, and RING) except the PHD, which is known to be used for the interaction with DPPA3 [18, 19] (Fig. 2B and C, Supplementary Material, Fig. S2A). The interaction between UHRF1 and NLRP5 or OOEP was retained under a high-stringent condition (Supplementary Material, Fig. S2B). In contrast to UHRF1, DNMT1, a maintenance DNA methyltransferase that

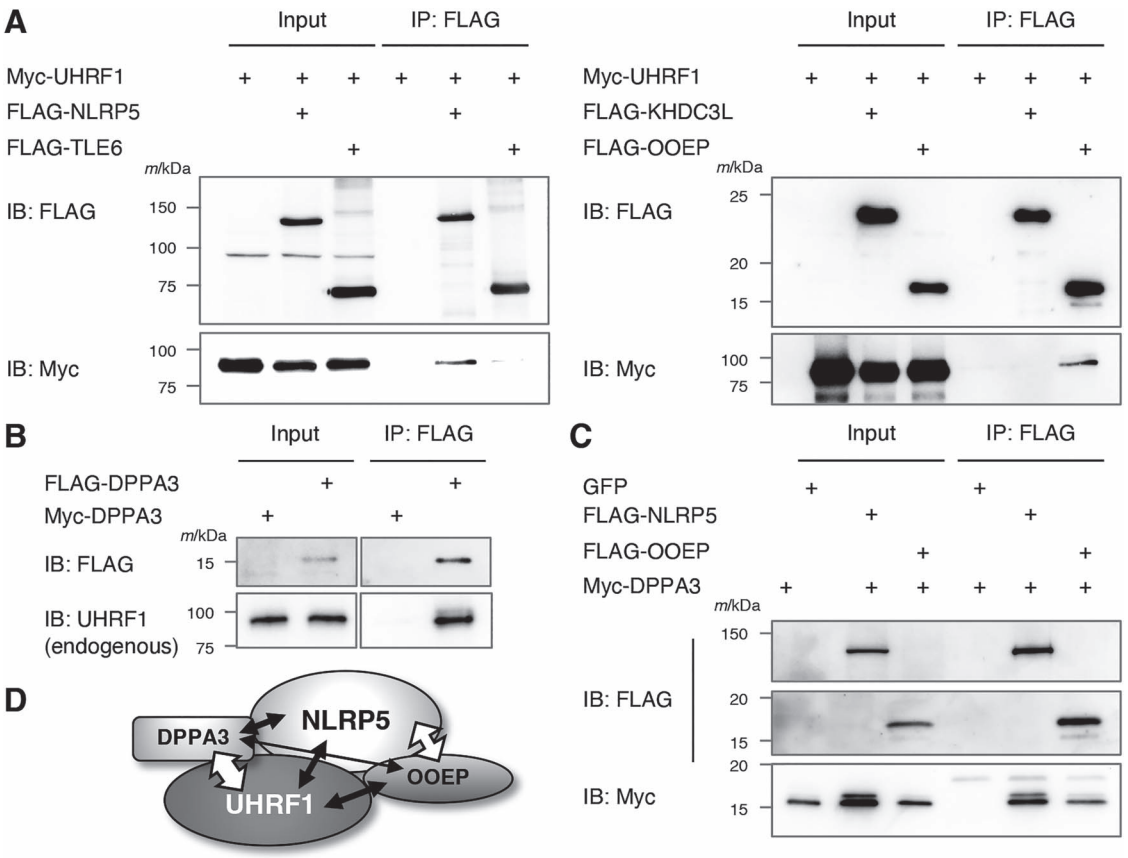

Figure 1. Interactions among human UHRF1, NLRP5, OOEP, and DPPA3. (A) Myc-tagged UHRF1 and FLAG-tagged NLRP5, TLE6, KHDC3L, and OOEP were co-expressed in HEK293T cells. Immunoprecipitation was performed using FLAG affinity gel. Indicated antibodies were used for western blotting. (B) FLAG-tagged or Myc-tagged DPPA3 were expressed in HEK293T cells. Immunoprecipitation was performed using FLAG affinity gel. Indicated antibodies were used for western blotting. (C) FLAG-NLRP5 and FLAG-OOEP were co-expressed with Myc-DPPA3 in HEK293T cells. Immunoprecipitation was performed using FLAG affinity gel. Indicated antibodies were used for western blotting. (D) Interactions among UHRF1, NLRP5, OOEP, and DPPA3. White arrows indicate previously reported interactions [15, 18, 19, 26], and black arrows indicate the interactions detected in this study.

functions with UHRF1, did not interact with the four SCMC components (Supplementary Material, Fig. S3).

Since OOEP is a small protein (predicted molecular mass is 17.2 kDa) with no predicted domains, we focused on determining a UHRF1 interacting domain(s) in NLRP5 protein, which is composed of a Pyrin-NALPs (Pyr) domain, a NACHT domain, and leucine-rich repeats (LRRs). To mimic subcellular localization of UHRF1 in oocytes and preimplantation embryos [2], we modified UHRF1 by adding a nuclear export signal (NES) [20] at its N-terminal and destroying a nuclear localization signal (NLS) in linker 4 (Supplementary Material, Fig. S4A). This modified protein was successfully localized in the cytoplasm (Supplementary Material, Fig. S4A–C), and thus we named the modified UHRF1 as cytoplasmic UHRF1 (cUHRF1). Intriguingly, FLAG-NLRP5 also interacts with Myc-cUHRF1 via its multiple domains, the NACHT domain and LRRs (Fig. 2A right and D), both of which are conserved in humans and mice [11]. Of note, pathogenic variants are found in these interaction sites in patients with MLID and female infertility (Supplementary Material, Fig. S5A and B). Further, we found that both the NACHT domain and LRRs of NLRP5 interact with the UBL, TTD, SRA, and RING domains of UHRF1 (Fig. 2E and F). The interaction mode between UHRF1 and NLRP5 is similar between UHRF1 and NLRP14, which has recently been reported to interact with UHRF1 protein in oocytes and preimplantation embryos [21, 22]; while UHRF1 interacts with NLRP14 via at least with the UBL and RING, but not via the PHD, NLRP14 interacts with UHRF1 via its NACHT and LRRs.

NLRP5 stabilizes UHRF1 in the cytoplasm

We next generated doxycycline (Dox)-inducible cUHRF1 T-REx-293 cells stably expressing FLAG-NLRP5 (Dox-cUHRF1 + NLRP5) or FLAG-OOEP (Dox-cUHRF1 + OOEP) to examine the effect of the presence of these proteins on the stability of cUHRF1 (Supplementary Material, Fig. S6A and B). Myc-cUHRF1 induced by Dox and FLAG-NLRP5 and FLAG-OOEP were well co-localized in the cytoplasm of these cell lines (Fig. 3A, Supplementary Material, Fig. S6C). We induced cUHRF1 by Dox in these cell lines, washed the cells with phosphate-buffered saline (PBS), and harvested the cells at 0, 24, 48, and 72 h (Fig. 3A). *cUHRF1* mRNA expression levels in Dox-cUHRF1, Dox-cUHRF1 + NLRP5, and Dox-cUHRF1 + OOEP cell lines were reduced to around basal level by 48 h with almost the same kinetics (Fig. 3B). Although the presence of OOEP did not affect cUHRF1 protein stability, cUHRF1 protein was significantly stabilized in the presence of NLRP5 (Fig. 3C and D). The average of the estimated protein half-life of cUHRF1 in the absence and presence of NLRP5 was 42.0 h and 100.1 h, respectively. This result suggests that NLRP5 stabilizes UHRF1 in the cytoplasm possibly via the protein–protein interaction.

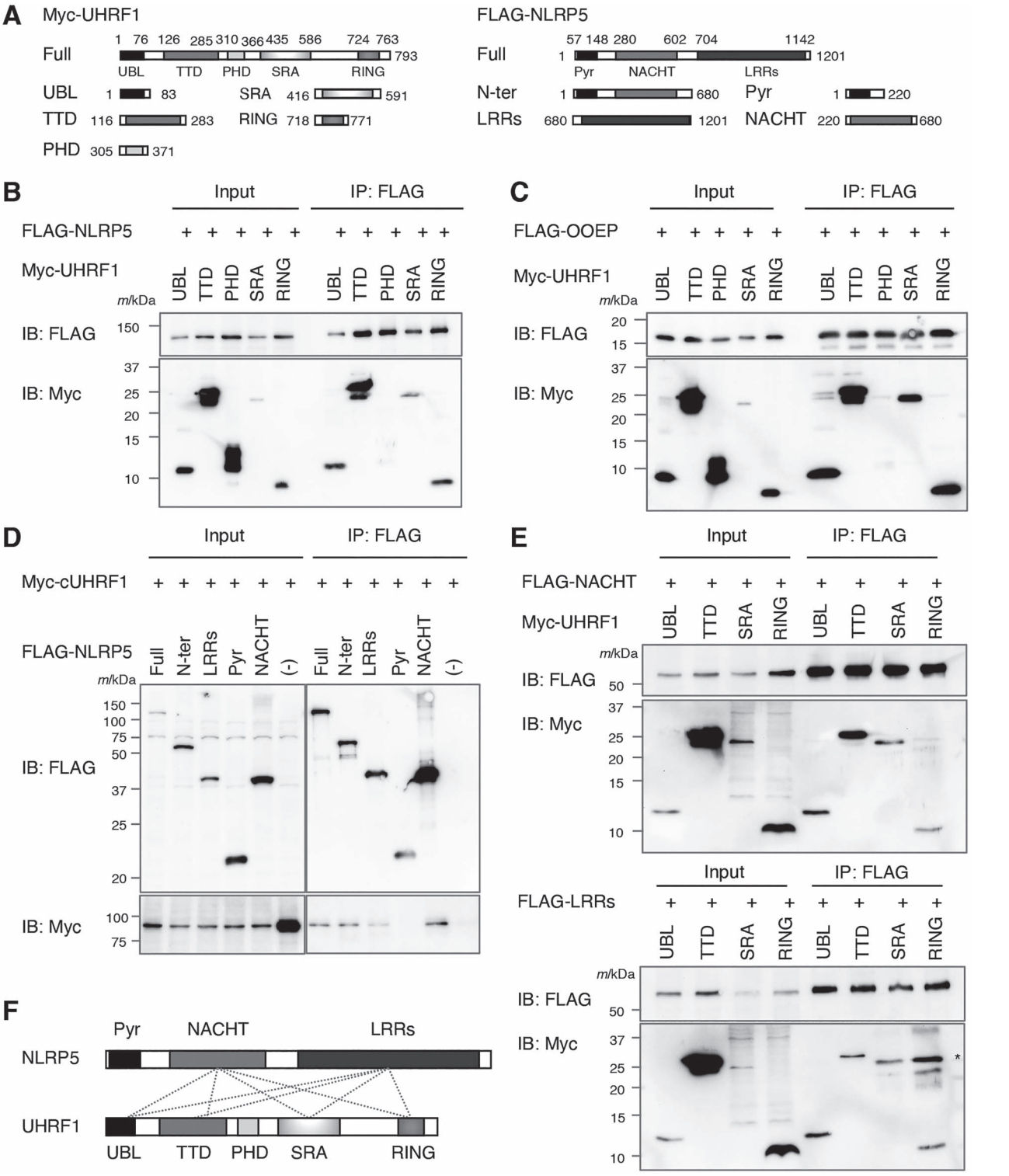

Figure 2. Human UHRF1 interacts with NLRP5 and OOEP via its multiple domains. (A) Plasmid constructs for expressing domains of UHRF1 (left) and NLRP5 (right). UBL, ubiquitin-like; TTD, tandem Tudor domain; PHD, plant homeodomain; SRA, SET and RING-associated; RING, really interesting new gene; Pyr, Pyrin-NALPs; LRRs, leucine repeats. (B and C) Myc-tagged UBL, TTD, PHD, SRA, and RING domains of UHRF1 were co-expressed with FLAG-NLRP5 (B) or FLAG-OOEP (C) in HEK293T cells. Immunoprecipitation was performed using FLAG affinity gel. Indicated antibodies were used for western blotting. (D) Myc-cUHRF1 and FLAG-NLRP5 mutants were co-expressed in HEK293T cells. Immunoprecipitation was performed using FLAG affinity gel. Indicated antibodies were used for western blotting. (E) Myc-UHRF1 domains and FLAG-NACHT or FLAG-LRRs were co-expressed in HEK293T cells. Immunoprecipitation was performed using FLAG affinity gel. Indicated antibodies were used for western blotting. *, IgG. (F) Schematic summary of the interactions between NLRP5 and UHRF1. The gray dotted lines indicate the identified interactions by immunoprecipitation in this study.

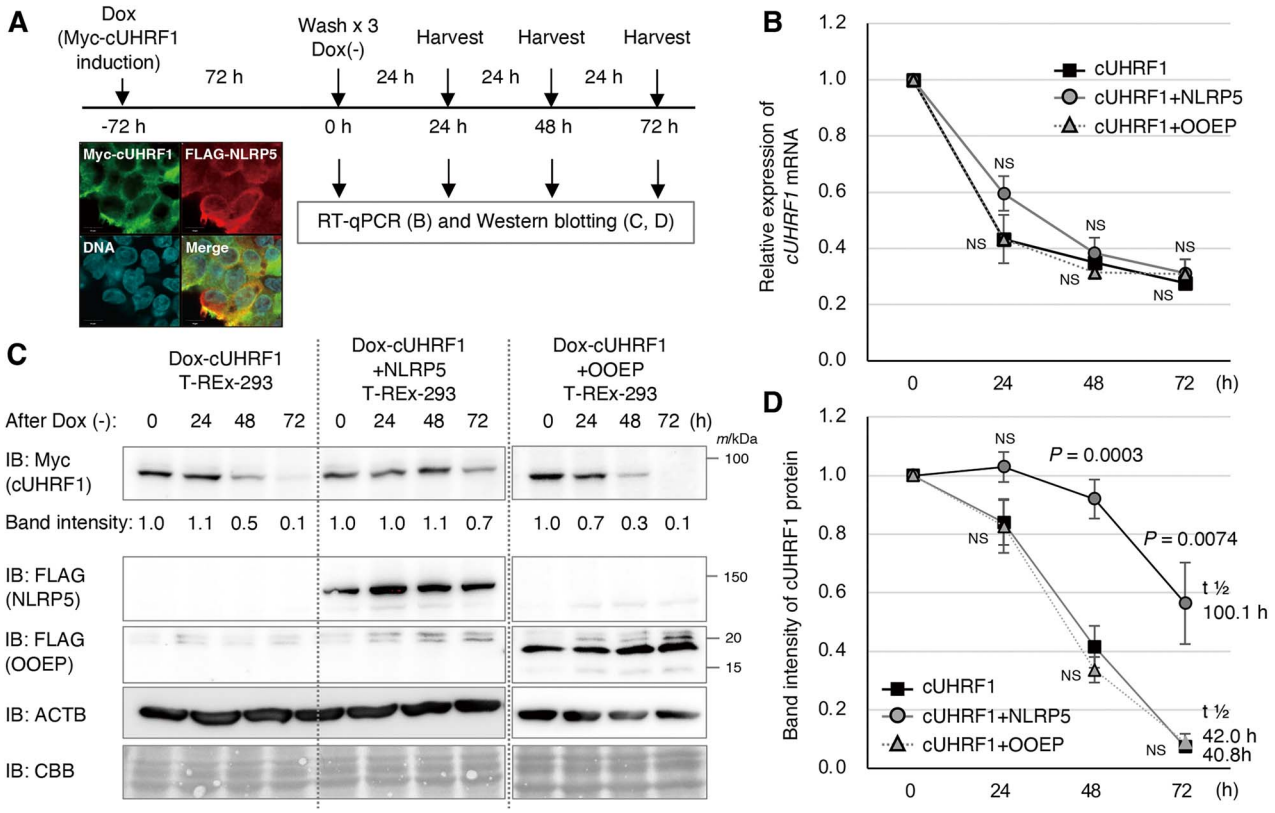

Figure 3. NLRP5 stabilizes UHRF1 protein in the cytoplasm. (A) Dox-inducible Myc-cytoplasmic UHRF1 (cUHRF1) T-REx-293 (Dox-cUHRF1) and Dox-inducible Myc-cUHRF1 T-REx-293 stably expressing FLAG-NLRP5 (Dox-cUHRF1 + NLRP5) or FLAG-OOEP (Dox-cUHRF1 + OOEP) were treated with Dox for 72 h to induce Myc-cUHRF1 (see Supplementary Material, Fig. S4 and S6). Then cells were washed three times and harvested for RT-qPCR and western blotting. A representative image of subcellular localization of Myc-cUHRF1 and FLAG-NLRP5 is shown (see Supplementary Material, Fig. S6). (B) Relative expression of *cUHRF1* mRNA in Dox-cUHRF1 (black rectangle), Dox-cUHRF1 + NLRP5 (gray circle), and Dox-cUHRF1 + OOEP (gray triangle) T-REx-293 cells was examined by RT-qPCR using a primer on *UHRF1* and another primer on the vector. *ACTB* was used for normalization. ΔΔCT was calculated compared with the expression of *cUHRF1* at 0 h. Experiments were performed in biological and technical triplicate (n = 9). Data are presented as the mean ± standard deviation (SD). NS, not significant by Student's t-test. (C) cUHRF1 protein levels in Dox-cUHRF1, Dox-cUHRF1 + NLRP5, and Dox-cUHRF1 + OOEP T-REx-293 cells were examined by western blotting using anti-Myc antibody to detect Myc-cUHRF1. A representative image of the experiment performed in biological and technical triplicate (n = 9) is shown. Anti-ACTB antibody was used for loading control, and anti-FLAG antibody was used to confirm the stable expression of FLAG-NLRP5 and FLAG-OOEP. Band intensity of cUHRF1 at 24, 48, and 72 h was calculated compared with that of cUHRF1 at 0 h. CBB, Coomassie Brilliant Blue. (D) Summary of western blotting results. The black rectangle, gray circle, and gray triangle indicate the relative expression of cUHRF1 protein in Dox-cUHRF1, Dox-cUHRF1 + NLRP5, and Dox-cUHRF1 + OOEP T-REx-293 cells, respectively. The estimated protein half-life (t 1/2) is indicated at right. Data are presented as the mean ± standard deviation (SD). *P*-values were obtained by Student's t-test. NS, not significant.

UHRF1 protein is decreased in murine *Nlrp5* KO FGOs

Finally, we generated *Nlrp5* KO mice using the CRISPR/Cas9 system (Fig. 4A). We confirmed that mouse NLRP5 was co-IPed with mouse UHRF1 by immunoprecipitation (Supplementary Material, Fig. S7A) despite low amino acid homology (51%) between mouse and human NLRP5 [11]. In contrast, physical interaction between UHRF1 and PADI6, one of the SCMC-associated proteins whose absence affects subcellular localization of UHRF1 in oocytes and preimplantation embryos [23], was barely detected (Supplementary Material, Fig. S7A). By immunofluorescence, we confirmed that NLRP5 protein was hardly detectable in *Nlrp5* KO FGOs (Fig. 4B). In the KO FGOs, the signal intensity of UHRF1 was significantly decreased in the cytoplasm, especially at the subcortical area (< 5 μm from membrane) (Fig. 4B and C). Of note, the signal intensity of UHRF1 is weak but detectable in the nucleus of wild-type (WT) FGOs, while it was significantly reduced in the nucleus of *Nlrp5* KO FGOs (Fig. 4C). The reduction of UHRF1 protein was unlikely a result of transcriptional suppression (Supplementary Material, Fig. S7B), thus it was likely a result of protein destabilization.

Discussion

In this study, we found that UHRF1 interacts with NLRP5 and OOEP, which are core components of the SCMC, via its multiple domains except for the PHD, and NLRP5 interacts with UHRF1 via its NACHT and LRRs. We also found that NLRP5 and OOEP interact with DPPA3, which exports UHRF1 from the nucleus to the cytoplasm during oocyte growth. Since the PHD of UHRF1 is essential for interacting with DPPA3 [18], UHRF1 seems to interact with DPPA3, NLRP5, and OOEP via different interacting interfaces. Recently, it has been reported that CTLs are composed of SCMC proteins and store UHRF1 in murine and human oocytes for the normal development of the early embryos [10]. This suggests that the interactions of these proteins detected in this study could occur at a high incidence in oocytes and preimplantation embryos. A more recent study revealed that murine NLRP5, possessing more than 10 LRRs, forms a homodimer via its two of the multiple LRRs, and interacts with OOEP and TLE6 via its NACHT domain and/or limited LRRs [24]. We hypothesize that NLRP5 could also interact with UHRF1 *in vivo* where NLRP5 is a part of CTLs formed by the SCMC through a different region(s) of the NACHT domain and/or a different LRR(s), distinct from those

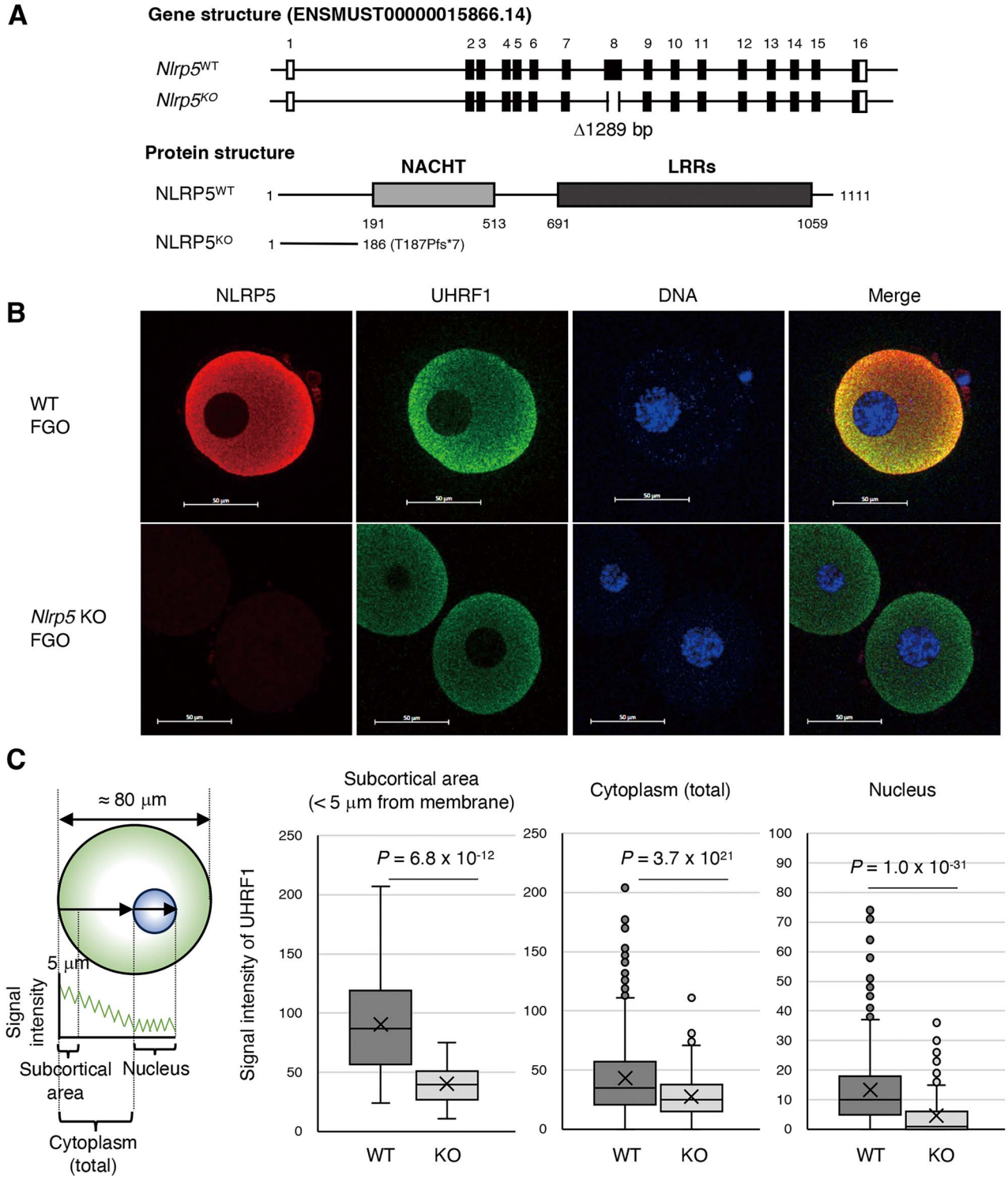

Figure 4. UHRF1 protein was destabilized in *Nlrp5* KO murine fully grown oocytes (FGOs). (A) Gene (transcript ID: ENSMUST00000015866.14) and protein structure of NLRP5 in wild-type (WT) and *Nlrp5* KO mice. Boxes in gene structure indicate exons, with black indicating coding regions. Gray and black boxes in protein structure indicate the NACHT domain and LRRs, respectively. The knockout mice possess a total of 1289 bp deletion in exon 8, resulting in a truncated protein (T187Pfs*7). (B) Representative image of subcellular localization of NLRP5 and UHRF1 in WT and *Nlrp5* KO FGOs. DNA was stained by DAPI. Scale bars: 50 μm. (C) Signal intensities of UHRF1 in WT and *Nlrp5* KO FGOs (n = 5 for each) were obtained using the profile function of the Zeiss ZEN 3.6 software. Each box indicates the 25th to 75th percentile, with a bar in the box indicating the median. "x" indicates the mean. *P*-values were obtained using the Wilcoxon signed-rank test.

involved in the homodimerization and interaction with OOEP and TLE6. We will determine the precise interaction sites between NLRP5 and UHRF1 as a next subject to pursue.

It has been enigmatic that the majority of DPPA3 relocates in the nucleus of GV oocytes, leaving UHRF1 in the cytoplasm [17]. Considering the interactions found in this study, we propose the

following model: In normal oocytes, DPPA3 exports UHRF1 from the nucleus to the cytoplasm and hands it over to NLRP5 and OOEP, resulting in the stable retention of UHRF1 on CTLs in the cytoplasm (Supplementary Material, Fig. S8A). Since depletion of any SCMC core protein leads to reduced protein stability of the other SCMC proteins including NLRP5, UHRF1 could be destabilized both in the cytoplasm and nucleus in oocytes of patients who carry pathogenic variants in the SCMC proteins in many cases. The reduced amount of UHRF1 in the nucleus can cause a defect in the maintenance of methylation of the CpGs in the ICRs during preimplantation development. This can cause MLID in relatively mild cases and embryonic death in severe cases, which manifests as female infertility (Supplementary Material, Fig. S8B), although other defects such as disruption of CTLs may be the major cause of the phenotype in the severe cases.

This hypothesis is based on our observation that UHRF1 protein in the nucleus is decreased in *Nlrp5* KO oocytes. However, although PADI6 and NLRP14 are SCMC-associated proteins, the levels of UHRF1 in the nucleus of their mutant oocytes and preimplantation embryos are increased, despite UHRF1 being decreased in the cytoplasm. This could plausibly lead CpG hypermethylation in these embryos [23, 25]. Thus, the reduction of UHRF1 in the cytoplasm of oocytes and preimplantation embryos seems not always to result in a reduction of the protein in the nucleus. It could be possible that in oocytes and preimplantation embryos, NLRP5 contributes to the stability of UHRF1, which is retained after relocation to the nucleus, possibly via a posttranslational modification(s), or to the maintenance of the nuclear amount of UHRF1 by influencing the interaction of proteins involved in nuclear import/export of UHRF1 such as DPPA3. We would like to identify the factor(s) as another future subject to pursue. Although further analyses proposed above are required, we believe that our findings contribute to fully understanding the pathogenesis of MLID caused by pathogenic variants of the cytoplasmic proteins, which have been a long-standing mystery.

Materials and methods

Ethics statement

Mouse husbandry and experiments were carried out in accordance with the ethical guidelines of Kyushu University, and the protocols were approved by the Animal Experiment Committee of Kyushu University.

Cell lines

HEK293T cells were obtained from the American Type Culture Collection, and Flp-In T-REx-293 cells were obtained from Thermo Fisher Scientific. Both cell lines were maintained in Dulbecco's modified Eagle's medium (Nacalai tesque) supplemented with 10% fetal bovine serum (FBS) and penicillin/streptomycin at 37°C and 5% CO_2.

Animals

We generated heterozygous *Nlrp5* KO mice with a total of 1289 bp deletion (1 bp deletion + 1288 bp deletion) in exon 8 of the *Nlrp5* gene (Transcript ID: ENSMUST00000015866.14), which encodes NLRP5_Thr187Profs*7, using the CRISPR/Cas9 system. Briefly, fertilized eggs obtained by crossing C57BL/6J females and males were electroporated with a mix of Cas9 Nuclease V3 (IDT) and guide RNA combined tracrRNA and crRNA (5′-*TGCTAAGTTCGACACAAGTG*-3′). The injected zygotes were transferred to the oviducts of pseudo-pregnant ICR females. Genotyping of the pups by PCR-based Sanger sequencing of tail-tip DNA identified a male carrying the deletion. This male was crossed with C57BL/6J females to confirm successful germline transmission, and the offspring carrying the mutation was further backcrossed to C57BL/6J mice. The mice were genotyped by PCR using the primers in Supplementary Material, Table S1. All control and KO mice were of the C57BL/6J background (*Mus musculus domesticus*). By crossing heterozygous KO females and heterozygous/homozygous KO males, both of which are fertile, we obtained homozygous KO females, which are viable but infertile. *Nlrp5* KO FGOs were obtained from the homozygous female mice.

Plasmids

Human *NLRP5* cDNA was synthesized by Eurofins Genomics and cloned into p3xFLAG–CMV-10 plasmid vector (Sigma-Aldrich). pCMV–HA human *OOEP*, pCMV–HA human *TLE6*, and pCMV–HA human *KHDC3L* plasmids [26] were kind gifts of Prof. Lei Li and Dr Dandan Qin (Institute of Zoology, Chinese Academy of Sciences) and pCS2 mouse *Padi6* plasmid was a kind gift from Dr Sugako Ogushi (Osaka University). We subcloned these cDNAs into p3xFLAG–CMV-10 vector. A series of EGFP-UHRF1 (full length, UBL, TTD, PHD, SRA, RING, and a series of domain deletion mutants) pEGFP-C2 vectors [27] were kind gifts from Prof. Pierre-Antoine Defossez (Université Paris Cité). We subcloned these cDNAs into pCMV–Myc vector (Clontech). We also subcloned human *DNMT1* cDNA in pFASTBac vector [28], which is a kind gift from Prof. Kyohei Arita (Yokohama City University) and human *DPPA3* cDNA in pVL1392-human DPPA3 WT vector, which is a kind gift from Dr Atsuya Nishiyama (the University of Tokyo), into pCMV–Myc vector (Clontech). The full length of mouse *Uhrf1* and *Nlrp5* cDNA was amplified by PCR using KOD One (TOYOKO) and cloned into pCMV–Myc and p3xFLAG–CMV-10 vectors, respectively.

We deleted 8 amino acids (667-674: KKTKVEPY) in NLS2 (663-674: RRTSKKTKVEPY) of UHRF1 in pCMV–Myc vector using PrimeSTAR Mutagenesis Basal Kit (TaKaRa Bio). Then we inserted a sequence of the second NES of the influenza A virus NS2 protein (MITQFESLKL encoded by 5′-*ATGATAACACAGTTCGAGTCACTGA AACTA*-3′) [20] between Myc and $UHRF1_{\Delta NLS2(667\text{-}674)}$ to obtain Myc-NES-$UHRF1_{\Delta NLS2(667\text{-}674)}$ expression plasmid. We named NES-$UHRF1_{\Delta NLS2(667\text{-}674)}$ as cytoplasmic UHRF1 (cUHRF1) and subcloned the *Myc-cUHRF1* cDNA into pcDNA5/FRT/TO vector (Thermo Fisher Scientific) for generating Dox-inducible Myc-cUHRF1 T-REx-293 cells.

Immunoprecipitation

HEK293T cells were harvested after 48 h of transfection and lysed in 0.5% NP-40 lysis buffer [150 mM NaCl, 0.5% NP-40, and 50 mM Tris–HCl (pH 8.0)]. Immunoprecipitation was performed as described previously [29]. Antibodies used for western blotting are listed in Supplementary Material, Table S2.

Examination of UHRF1 protein stability with or without NLRP5 and OOEP

A Dox-inducible cUHRF1 cell line was generated by transfection of Myc-cUHRF1 pcDNA5/FRT/TO plasmid into Flp-In T-REx-293 cells, which contain a single FRT site and stably expresses the Tet repressor (Thermo Fisher Scientific) according to the manufacturer's protocol. Myc-cUHRF1 expression was induced by Dox (0.5 μg/ml). By transfection of NLRP5 or OOEP p3xFLAG–CMV-10 plasmid into the cell line and subsequent Geneticin (600 μg/ml) selection, Dox-inducible Myc-cUHRF1 T-REx-293 cells stably expressing FLAG-NLRP5 or FLAG-OOEP were established from a single cell, respectively.

To examine the effect of the presence of NLRP5 and OOEP on the cUHRF1protein stability, Dox-inducible Myc-cUHRF1 T-REx-293 cells stably expressing FLAG-NLRP5 or FLAG-OOEP, as well as its parental cell line, were treated with Dox for three days. Then we washed the cells with PBS three times and suspended the cells in DMEM supplemented with 10% Tet System Approved FBS (TaKaRa Bio) and penicillin/streptomycin. Then cells were harvested at indicated times and served for Western blotting and quantitative PCR (qPCR). The experiments were performed in biological and technical triplicate. For Western blotting, cells were lysed in radioimmunoprecipitation assay (RIPA) buffer [150 mM NaCl, 1% NP40, 0.5% sodium deoxycholate, 0.1% sodium dodecyl sulfate (SDS), and 50 mM Tris–HCl (pH 8.0)] and performed western blotting using indicated antibodies (Supplementary Material, Table S2). The same amount of protein loading was confirmed by using anti-ACTB antibody, and also membrane staining by Coomassie Brilliant Blue (CBB) staining after Western blotting. Protein band intensity was obtained using iBright FL1500 Imaging System (Life Technologies). The estimated protein half-life of cUHRF1 was obtained by linear regression. For qPCR, total RNAs were extracted from cells using ISOGEN (Nippon Gene), and the cDNAs were generated using a PrimeScript RT reagent Kit with gDNA Eraser (TaKaRa Bio) according to the manufacturer's protocol. Primer sequences are listed in Supplementary Material, Table S1. PCR reactions were conducted using a CFX Connect Real-Time PCR Detection System (BioRad Laboratories) according to the manufacturer's protocol. Amplification conditions were 30 s at 95°C, followed by 40 cycles of 5 s at 95°C each, and then 30 s at 60°C. The *ACTB* mRNA levels were used for normalization. The mRNA abundance (ΔCt) of *cUHRF1* in 24, 48, and 72 h after Dox depletion was calculated by comparison with that of *ACTB* and was presented as relative to its expression level at 0 h (ΔΔCt).

Immunofluorescence

Immunofluorescence staining of FGOs was performed as follows. FGOs were fixed with 4% paraformaldehyde and permeabilized with 0.5% Triton X-100 in PBS for 30 min at room temperature. The cells were then incubated with primary antibodies (Supplementary Material, Table S2) at 4°C, overnight. After washing several times, the cells were incubated with secondary antibodies (Supplementary Material, Table S2) for 30 min at room temperature. After mounting in VECTASHIELD medium with DAPI (Vector Laboratory), the cells were observed using LSM700 confocal laser scanning microscope (Carl Zeiss).

Statistics

To determine the statistical significance of the data examining *cUHRF1* mRNA expression and protein stability (Fig. 3B and D), Student's t-test was performed. To examine UHRF1 protein levels in WT and *Nlrp5* KO murine FGOs (n = 5), signal intensities in each FGO were measured using the "profile" function of the Zeiss Zen 3.6 program. The analysis provided signal intensities at more than 80 points in the cytoplasm (total), more than 15 points at the subcortical area, and more than 47 points in the nucleus of each FGO. We compared the summed signal intensities of UHRF1 in five WT FGOs (cytoplasm, n = 643; subcortical area, n = 78; nucleus n = 438) and five *Nlrp5* KO FGOs (cytoplasm, n = 496; subcortical area, n = 78; nucleus, n = 366) using Wilcoxon signed-rank test using R (wilcox.test).

Acknowledgments

We thank Lei Li and Dandan Qin (Institute of Zoology, Chinese Academy of Sciences) for providing us pCMV-HA OOEP, pCMV-HA TLE6, and pCMV-HA KHDC3L plasmids, Pierre-Antoine Defossez (Université Paris Cité) for a series of EGFP-UHRF1 plasmids, Kyohei Arita (Yokohama City University) for pFASTBac-human DNMT1 WT plasmid and valuable discussion, Atsuya Nishiyama (the University of Tokyo) for pVL1392-human DPPA3 WT plasmid, Scott A. Coonrod (Baker Institute for Animal Health) for anti-NLRP5 antibody, and Sugako Ogushi (Osaka University) for pCS2-Padi6 plasmid. The authors thank the members of the Research Promotion Unit of the Medical Institute of Bioregulation, Kyushu University, for supporting the mouse experiments.

Supplementary data

Supplementary data is available at *HMG Journal* online.

Conflict of interest statement: The authors declare no competing interests.

Funding

This work was supported by Japan Society for Promotion of Science KAKENHI Grant no. JP19H05740, 13K05728, and 23K05728 (to M. U.) and JP18H05214 (to H. S.).

References

1. Hirasawa R, Chiba H, Kaneda M. *et al.* Maternal and zygotic Dnmt1 are necessary and sufficient for the maintenance of DNA methylation imprints during preimplantation development. *Genes Dev* 2008;**22**:1607–1616.
2. Maenohara S, Unoki M, Toh H. *et al.* Role of UHRF1 in de novo DNA methylation in oocytes and maintenance methylation in preimplantation embryos. *PLoS Genet* 2017;**13**:e1007042.
3. Unoki M, Sasaki H. The UHRF protein family in epigenetics, development, and carcinogenesis. *Proc Jpn Acad Ser B Phys Biol Sci* 2022;**98**:401–415.
4. Docherty LE, Rezwan FI, Poole RL. *et al.* Mutations in NLRP5 are associated with reproductive wastage and multilocus imprinting disorders in humans. *Nat Commun* 2015;**6**:8086.
5. Kagami M, Hara-Isono K, Matsubara K. *et al.* ZNF445: a homozygous truncating variant in a patient with temple syndrome and multilocus imprinting disturbance. *Clin Epigenetics* 2021;**13**:119.
6. Mackay DJ, Callaway JL, Marks SM. *et al.* Hypomethylation of multiple imprinted loci in individuals with transient neonatal diabetes is associated with mutations in ZFP57. *Nat Genet* 2008;**40**:949–951.
7. Begemann M, Rezwan FI, Beygo J. *et al.* Maternal variants in NLRP and other maternal effect proteins are associated with multilocus imprinting disturbance in offspring. *J Med Genet* 2018;**55**:497–504.
8. Tong X, Jin J, Hu Z. *et al.* Mutations in OOEP and NLRP5 identified in infertile patients with early embryonic arrest. *Hum Mutat* 2022;**43**:1909–1920.
9. Tong ZB, Gold L, Pfeifer KE. *et al.* Mater, a maternal effect gene required for early embryonic development in mice. *Nat Genet* 2000;**26**:267–268.
10. Jentoft IMA, Bauerlein FJB, Welp LM. *et al.* Mammalian oocytes store proteins for the early embryo on cytoplasmic lattices. *Cell* 2023;**186**:5308–5327.e25.
11. Lu X, Gao Z, Qin D. *et al.* A maternal functional module in the mammalian oocyte-to-embryo transition. *Trends Mol Med* 2017;**23**:1014–1023.
12. Uemura S, Maenohara S, Inoue K. *et al.* UHRF1 is essential for proper cytoplasmic architecture and function of mouse oocytes and derived embryos. *Life Sci Alliance* 2023;**6**:e202301904.

13. Tashiro F, Kanai-Azuma M, Miyazaki S. *et al.* Maternal-effect gene Ces5/Ooep/Moep19/Floped is essential for oocyte cytoplasmic lattice formation and embryonic development at the maternal-zygotic stage transition. *Genes Cells* 2010;**15**:813–828.
14. Zheng P, Dean J. Role of Filia, a maternal effect gene, in maintaining euploidy during cleavage-stage mouse embryogenesis. *Proc Natl Acad Sci USA* 2009;**106**:7473–7478.
15. Li L, Baibakov B, Dean J. A subcortical maternal complex essential for preimplantation mouse embryogenesis. *Dev Cell* 2008;**15**:416–425.
16. Yu XJ, Yi Z, Gao Z. *et al.* The subcortical maternal complex controls symmetric division of mouse zygotes by regulating F-actin dynamics. *Nat Commun* 2014;**5**:4887.
17. Li Y, Zhang Z, Chen J. *et al.* Stella safeguards the oocyte methylome by preventing de novo methylation mediated by DNMT1. *Nature* 2018;**564**:136–140.
18. Hata K, Kobayashi N, Sugimura K. *et al.* Structural basis for the unique multifaceted interaction of DPPA3 with the UHRF1 PHD finger. *Nucleic Acids Res* 2022;**50**:12527–12542.
19. Funaki S, Nakamura T, Nakatani T. *et al.* Inhibition of maintenance DNA methylation by Stella. *Biochem Biophys Res Commun* 2014;**453**:455–460.
20. Huang S, Chen J, Chen Q. *et al.* A second CRM1-dependent nuclear export signal in the influenza A virus NS2 protein contributes to the nuclear export of viral ribonucleoproteins. *J Virol* 2013;**87**:767–778.
21. Meng TG, Guo JN, Zhu L. *et al.* NLRP14 safeguards calcium homeostasis via regulating the K27 ubiquitination of Nclx in oocyte-to-embryo transition. *Adv Sci (Weinh)* 2023;**10**:e2301940.
22. Zhang W, Zhang R, Wu L. *et al.* NLRP14 deficiency causes female infertility with oocyte maturation defects and early embryonic arrest by impairing cytoplasmic UHRF1 abundance. *Cell Rep* 2023;**42**:113531.
23. Giaccari C, Cecere F, Argenziano L. *et al.* A maternal-effect Padi6 variant causes nuclear and cytoplasmic abnormalities in oocytes, as well as failure of epigenetic reprogramming and zygotic genome activation in embryos. *Genes Dev* 2024;**38**:131–150.
24. Chi P, Ou G, Qin D. *et al.* Structural basis of the subcortical maternal complex and its implications in reproductive disorders. *Nat Struct Mol Biol* 2024;**31**:115–124.
25. Yan R, Cheng X, Gu C. *et al.* Dynamics of DNA hydroxymethylation and methylation during mouse embryonic and germline development. *Nat Genet* 2023;**55**:130–143.
26. Zhu K, Yan L, Zhang X. *et al.* Identification of a human subcortical maternal complex. *Mol Hum Reprod* 2015;**21**:320–329.
27. Ferry L, Fournier A, Tsusaka T. *et al.* Methylation of DNA ligase 1 by G9a/GLP recruits UHRF1 to replicating DNA and regulates DNA methylation. *Mol Cell* 2017;**67**:550–565.e5.
28. Kikuchi A, Onoda H, Yamaguchi K. *et al.* Structural basis for activation of DNMT1. *Nat Commun* 2022;**13**:7130.
29. Unoki M, Funabiki H, Velasco G. *et al.* CDCA7 and HELLS mutations undermine nonhomologous end joining in centromeric instability syndrome. *J Clin Invest* 2019;**129**:78–92.